

An Investigation on the Potential of KAN in Speech Enhancement

Haoyang Li, Yuchen Hu, Chen Chen, Eng Siong Chng

Nanyang Technological University, College of Computing and Data Science, Singapore

Abstract

High-fidelity speech enhancement often requires sophisticated modeling to capture intricate, multiscale patterns. Standard activation functions, while introducing nonlinearity, lack the flexibility to fully address this complexity. Kolmogorov-Arnold Networks (KAN), an emerging methodology that employs learnable activation functions on graph edges, present a promising alternative. This work investigates two novel KAN variants based on rational and radial basis functions for speech enhancement. We integrate the rational variant into the 1D CNN blocks of Demucs and the GRU-Transformer blocks of MP-SENNet, while the radial variant is adapted to the 2D CNN-based decoders of MP-SENNet. Experiments on the VoiceBank-DEMAND dataset show that replacing standard activations with KAN-based activations improves speech quality across both the time-domain and time-frequency domain methods with minimal impact on model size and FLOP, underscoring KAN’s potential to improve speech enhancement models.

Index Terms: Speech Enhancement, Kolmogorov-Arnold Networks.

1. Introduction

Speech enhancement reduces noise and distortion to improve speech clarity, aiding applications like hearing aids, telecommunications and voice recognition systems. Deep learning-based speech enhancement (SE) methods can be generally classified under time domain methods [1] [2] [3] [4] [5] and time-frequency (TF) domain methods [6] [7] [8] [9] [10]. Time-domain methods aim to predict clean waveform directly from noisy counterparts. SEGAN [1] is trained in an adversarial manner with a CNN-based auto-encoder as the enhancement module. DEMUCS [2] combined a convolutional encoder-decoder with LSTM layers for effective sequential modeling. On the other hand, TF-domain methods predict clean TF-domain representation and recover time domain waveform from it. Some early TF-domain SE focused solely on enhancing the magnitude spectrum, followed by reconstructing clean speech using the Inverse Short-Time Fourier Transform (ISTFT) [6] [11]. Later approaches, such as CMGAN [7] and MP-SENNet [12], implicitly or explicitly predict clean phase information in addition to the magnitude spectrum, yielding better enhancement results. Advancements have also been made in designing better objective functions for SE. Early works [13] [14] typically minimize the L1/L2 distance of time-domain waveform or TF-domain representations, which does not precisely reflect human auditory perception. Metricgan [6] addresses the problem through optimizing the model on PESQ [15] or STOI [16] directly through GAN training with the discriminator serving as a PESQ/STOI score estimator.

Despite advancements in SE methods, current approaches typically rely on standard activation functions like GELU [17],

Swish [18], ReLU, PReLU and Leaky ReLU. While effective in general, these functions may limit the ability to fully capture the complex non-linear patterns in audio data, such as harmonic structures and phase variations, which are known to be challenging to model effectively [19] [20]. For instance, ReLU, Leaky ReLU and PReLU are piecewise linear, making them struggle with subtle variations in smooth curves like sine [21]. Swish, despite its smoothness, has a higher computational cost and does not consistently outperform ReLU [21]. Recently, KAN [22], which employ learnable activation functions on the edges of neural network graphs, have gained attention as a competitive alternative to MLP. Empirical studies in various domains, including computer vision [23], time series forecasting [24] and high-dimensional data handling [25] have demonstrated the superior modeling capability of KAN compared to MLP.

While a recent work [26] has shown that KAN can improve the performance of the TF-domain Metricgan+ [11], KAN’s potential in time-domain SE remains unexplored. Furthermore, the investigated MetricGAN+ operates solely on the magnitude spectrum, which underperforms significantly to SoTA TF-domain methods that enhance both magnitude and phase spectrum jointly [7] [12].

In this study, we bridge these gaps by adapting KAN to two distinct SE paradigms: Demucs [2], a time-domain SE model, and MP-SENNet [12], a SoTA TF-domain SE model that jointly enhances magnitude and phase. Our findings demonstrate that KAN activations based on rational functions improve the performance of 1D CNN blocks in Demucs and GRU-Transformer blocks in MP-SENNet, yielding PESQ gains from 2.896 to 2.990 and 3.555 to 3.572, respectively, with minimal increases in model size and computational cost. Additionally, we found that KAN-Conv2D blocks based on radial basis functions outperform Conv2D blocks based on standard activation functions, further improving the PESQ of MP-SENNet from 3.572 to 3.609. Notably, the KAN variants proposed in this work based on rational and radial basis functions differ from the previous work [26], further underscoring the versatility of KAN activations in SE. Our findings highlight the potential of KAN based activation functions as robust alternatives to conventional activation functions in SE models, advancing the field beyond the current SoTA.

2. Preliminaries

2.1. KAN: Kolmogorov-Arnold Network

KAN is developed based on the Kolmogorov-Arnold theorem [27], which asserts that any continuous function can be represented as a composition of univariate continuous functions of a finite number of variables. In theory, each KAN layer L is a composition of learnable univariate functions ϕ as illustrated in equation 1, where I and O are the input and output dimensions. These univariate functions can be used to model contin-

uous functions.

$$L(\mathbf{x}) = \Phi \circ \mathbf{x} = \left[\sum_{i=1}^I \phi_{i,1}(x_i) \quad \dots \quad \sum_{i=1}^I \phi_{i,O}(x_i) \right],$$

$$\text{where } \Phi = \begin{bmatrix} \phi_{1,1}(\cdot) & \phi_{1,2}(\cdot) & \dots & \phi_{1,I}(\cdot) \\ \phi_{2,1}(\cdot) & \phi_{2,2}(\cdot) & \ddots & \vdots \\ \vdots & \vdots & \ddots & \vdots \\ \phi_{O,1}(\cdot) & \dots & \dots & \phi_{O,I}(\cdot) \end{bmatrix} \quad (1)$$

In practice, a KAN layer L is approximated by equation 2 for efficiency gain, where w_1 and w_2 are learnable scaler, b is a basis function such as Swish, serving a role similar to residual connections. *spline* is a B-spline function, which uses a series of lower-degree polynomial segments to represent smooth curve with high degree of polynomial.

$$L(\mathbf{x}) = w_1 b(x) + w_2 \text{spline}(x) \quad (2)$$

2.2. GR-KAN: KAN variant based on rational functions

[28] proposes replacing B-spline with rational function due to the later's greater efficiency and modeling capacity. To further reduce the parameter count, [28] splits the I input channels into k groups, and share the parameters of the rational functions across all channels in the same group. Specifically, a GR-KAN layer is represented by equation 3, where ϕ is now rational function, I/k is the dimension size per group, and w are unique scalars. The authors also proposed a variance-preserving initialization strategy to mimic specific behaviors such as Swish or identity functions for better training stability.

$$\begin{aligned} L(\mathbf{x}) &= \Phi \circ \mathbf{x} \\ &= \left[\sum_{i=1}^I w_{i,1} \phi_{\lfloor \frac{i}{I/k} \rfloor}(x_i) \quad \dots \quad \sum_{i=1}^I w_{i,O} \phi_{\lfloor \frac{i}{I/k} \rfloor}(x_i) \right] \end{aligned} \quad (3)$$

2.3. RBF-KAN: KAN variant based on radial basis functions

[29] proposes using radial basis function (RBFs) as another alternative to B-spline to improve computational efficiency. RBFs are a type of real-valued function that derive their values exclusively from the distance to a specific central point, and are shown to be able to approximate 3-order B-spline bases accurately [29]. In other words, $w_2 \text{spline}(x)$ from equation 2 can be approximated by equation 4 below, where C is the number of centers, w_i are learnable weights, c_i are the centers and ϕ is the radial basis function. In [29], the radial basis function is a Gaussian function as illustrated in equation 5, where s controls the width of the function.

$$\text{RBF}(x) = \sum_{i=1}^C w_i \phi(\|x - c_i\|) \quad (4)$$

$$\phi(\|x - c_i\|) = \exp\left(-\frac{(x - c_i)^2}{2s^2}\right) \quad (5)$$

3. KAN in Speech Enhancement

3.1. KAN in Time-domain SE

We first investigate the impact of KAN activation on time-domain SE. Figure 1 illustrates the GR-KAN adapted causal Demucs, where we replace the ReLU activations in the original

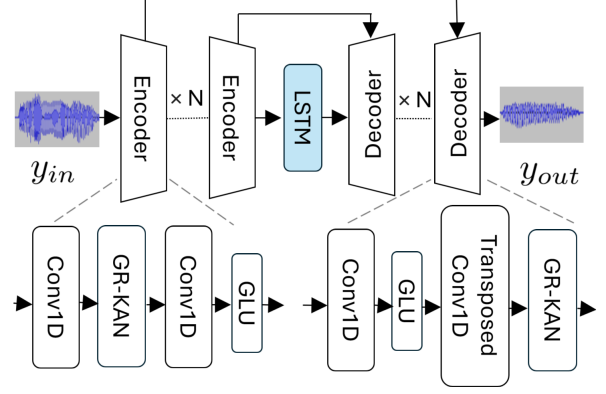


Figure 1: Architecture of Causal Demucs, where we replace all Relu activations in the Encoders and Decoders with GR-KAN activations. Please note that the last Decoder does not have the GR-KAN activation.

Encoders and Decoders with GR-KAN activations. Unlike the original GR-KAN implementation which sends the output of the rational functions to a linear layer to learn the scaling factors w in equation 3, we send the output of the rational functions to the subsequent 1D CNN layer.

For comparative analysis, we implemented several other model variants in which we only adapted GR-KAN to the encoders or the decoders, or we do not use GR-KAN at all. We also investigated the impact on model performance when there are changes in the number of groups k for parameter sharing in the GR-KAN layers.

3.2. KAN in T-F domain SE

We also investigate the impact of KAN on the TF-domain MP-SENNet. Figure 2a illustrate the overall architecture of the KAN adapted model. The power-law compressed magnitude spectrum $Y_m \in \mathbb{R}^{T \times F}$ and the wrapped phase spectrum $Y_p \in \mathbb{R}^{T \times F}$, where T and F are the number of time frames and frequency bins, respectively, are stacked to form the model input $Y_{in} \in \mathbb{R}^{T \times F \times 2}$. The encoder takes in Y_{in} followed by a stack of N TF-Transformer blocks to capture local and global dependencies. Within each TF-Transformer block, the first GRU-Transformer block captures dependency across the time dimension by rearranging the input matrix to (BF', T, C) and the second GRU-Transformer block captures dependency across the frequency dimension by rearranging the input matrix to (BT, F', C) . We use F' here instead of F because the encoder compresses the frequency dimension F by a factor of 2 (i.e. $F' = F/2$). The output of the last TF-Transformer block is fed into a Magnitude Decoder and a Phase Decoder separately to restore the enhanced, power-law compressed magnitude spectrum $\hat{X}_m \in \mathbb{R}^{T \times F}$ and the enhanced phase spectrum $\hat{X}_p \in \mathbb{R}^{T \times F}$.

The architecture of the KAN-adapted GRU-Transformer block is illustrated in figure 2b. After undergoing sequential processing through a multi-head-self attention and a bi-directional GRU layer, the sequence is further processed through 2 GR-KAN activations, each followed by a linear layer. We follow [28] to initialize the first GR-KAN with identity matrix and the second GR-KAN with GELU. For comparative analysis, we also implemented 3 other GRU-Transformer block variants without GR-KAN. The first 2 variants replace the GR-KAN activations in figure 2b with GELU and Leaky

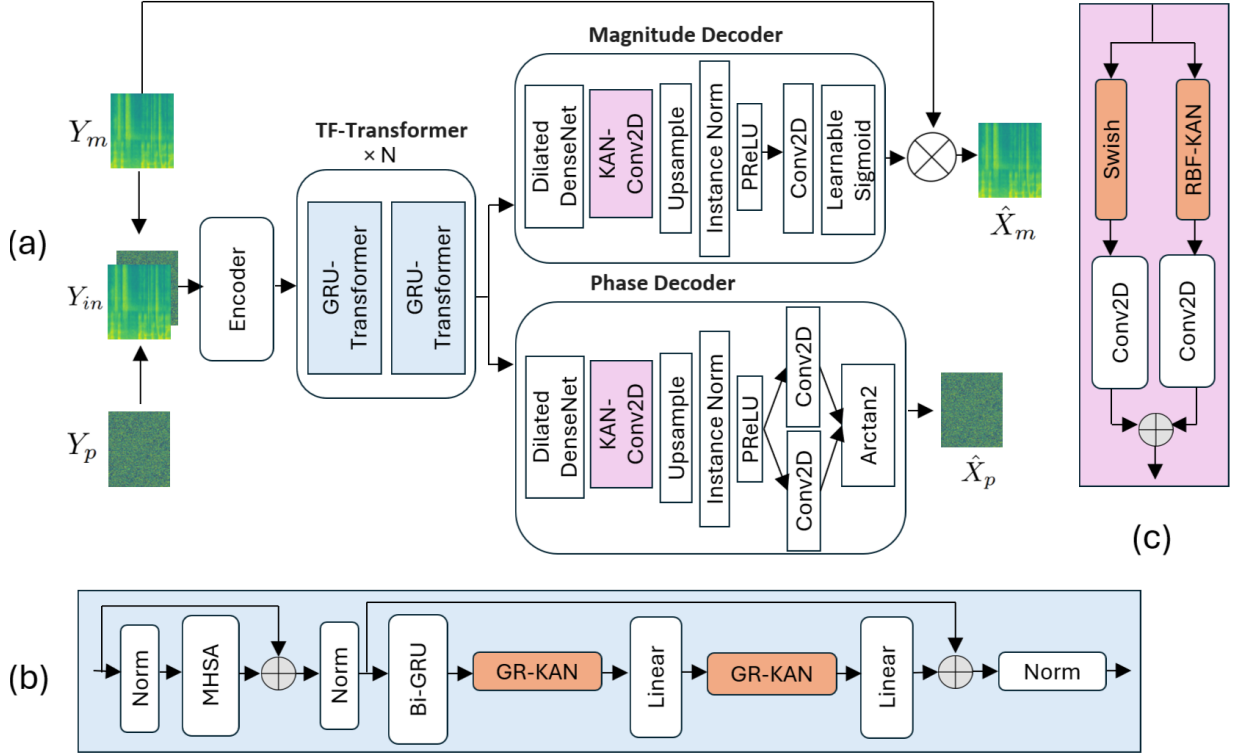


Figure 2: Architecture of the (a) KAN adapted MP-SENet (b) KAN adapted GRU-Transformer Block (c) KAN-Conv2D Block.

ReLU activations, respectively. The last variant is the original GRU-Transformer block in MP-SENet, where we replace the $linear(GR-KAN(linear(GR-KAN(x))))$ after the Bi-GRU with $linear(leakyReLU(x))$.

To further integrate KAN into MP-SENet, we place a KAN-Conv2D module in the Magnitude Decoder and the Phase Decoder. As illustrated in figure 2c, the implementation of the KAN-Conv2D module follows KA-Conv¹, which contains two Conv2D layers arranged in parallel. For one branch, the Conv2D layer is preceded by a RBF-KAN activation, and the other is preceded by a Swish activation. The output of the Conv2D layers are merged through addition. Similar to the original MP-SENet, KAN-Conv2D is used to expand the channel dimension of the input by a factor of 2 while maintaining the spatial resolution. This allows the subsequent Upsample module to expand the frequency dimensions from F' to F by rearranging the expanded channel dimensions. For comparative analysis, we also implemented 2 other decoder variants without RBF-KAN. The first replaces the RBF-KAN activation in KAN-Conv2D with Swish activation. The second follows the original MP-SENet, where we replace KAN-Conv2D with PReLU followed by a standard Conv2D layer.

4. Experiments

4.1. Dataset

We investigate our solutions using VoiceBank-DEMAND [30], a widely recognized benchmark dataset for SE. The training set comprises 11,572 clean utterances from 28 speakers, while the test set consists of 824 clean utterances from 2 unseen speakers, all originating from the Voice Bank corpus [31]. Each clean

utterance is paired with a corresponding noisy version. In the training set, the noise is sourced from 8 types of noise in the DEMAND database [32] and 2 types of artificial noise, with SNRs of 0 dB, 5 dB, 10 dB, and 15 dB. For the test set, 5 unseen noise types from the DEMAND database are used, with SNRs of 2.5 dB, 7.5 dB, 12.5 dB, and 17.5 dB. We down-sampled all audio clips to 16kHz.

4.2. Experimental Setup

For Demucs, we used the causal version with 5 encoder blocks, 5 decoder blocks and a 2 layer unidirectional LSTM. We set the initial hidden dimension to 48, kernel size to 8, stride size and resample factor to 4. All models are trained to 500 epochs using the adam optimizer at a learning rate of 0.0003 and batch size of 16. The model is optimized using L1 loss on the waveform and a multi-resolution STFT loss on the magnitude spectrum.

For MP-SENet, we used a hop size, Hanning window size and FFT point number of 100, 400 and 400, respectively. We trained all models to 200 epochs with a batch size of 4 using the AdamW optimizer [33] with $\beta_1 = 0.8$ and $\beta_2 = 0.99$. We set the learning rate to 0.0005, which decays with a factor of 0.99 every epoch. Our training objective follows MP-SENet, where the generator is optimized using a weighted sum of the magnitude spectrum loss, phase spectrum loss, complex spectrum loss, STFT consistency loss and metricgan loss, while the discriminator is trained to predict the PESQ of the predicted magnitude spectrum.

4.3. Evaluation Metrics

Following [6] [11] [7] [20], we evaluate our models with PESQ [15], CSIG, CBAK, COVL [34] and STOI [16], which are measurements for perceptual speech quality, signal distortion, noise

¹<https://github.com/XiangboGaoBarry/KA-Conv>

Table 1: Comparison of GR-KAN and ReLU activation in Demucs

KAN Encoder	KAN Decoder	Group Size	PESQ	CSIG	CBAK	COVL	STOI	GFLOPs	#P (M)
N	N	-	2.896	4.284	3.429	3.608	0.945	18.868	43.083
Y	N	8	2.970	4.330	3.472	3.674	0.948	18.868	43.395
Y	N	16	2.909	4.314	3.472	3.632	0.946	18.868	43.395
Y	N	24	2.975	4.348	3.498	3.683	0.947	18.868	43.395
N	Y	8	2.950	4.320	3.471	3.657	0.946	18.868	43.385
N	Y	16	2.934	4.324	3.446	3.650	0.946	18.868	43.385
N	Y	24	2.990	4.349	3.495	3.695	0.947	18.868	43.385
Y	Y	24	2.987	4.342	3.500	3.688	0.947	18.869	43.698

Table 2: Comparison of GR-KAN and standard activations in MP-SENet

Activation	PESQ	CSIG	CBAK	COVL	STOI	GFLOPs	#P (M)
LeakyReLU*	3.555	4.692	3.915	4.204	0.958	387	2.26
LeakyReLU	3.563	4.709	3.891	4.216	0.960	392	2.30
GELU	3.565	4.707	3.921	4.214	0.960	397	2.30
GR-KAN	3.572	4.720	3.918	4.225	0.961	401	2.30

Table 3: Comparison of RBF-KAN and standard activations in MP-SENet

Activation	PESQ	CSIG	CBAK	COVL	STOI	GFLOPs	#P (M)
PReLU (Conv2D)	3.572	4.720	3.918	4.225	0.961	401	2.30
Swish+Swish (KAN-Conv2D)	3.537	4.695	3.882	4.191	0.960	409	2.35
RBF-KAN+Swish (KAN-Conv2D)	3.609	4.733	3.923	4.252	0.961	433	2.49

Table 4: Comparison between our work and other SE solutions

Method	Input	PESQ	CSIG	CBAK	COVL	STOI
Noisy	-	1.97	3.35	2.44	2.63	0.91
SEGAN	Time	2.16	3.48	2.94	2.80	0.92
MetricGAN	Magnitude	2.86	3.99	3.18	3.42	-
DEMUCS	Time	1.28	4.31	3.40	3.63	0.95
MetricGAN+	Magnitude	3.15	4.14	3.16	3.64	-
SE-Conformer	Time	3.13	4.45	3.55	3.82	0.95
CMGAN	Complex+Magnitude	3.41	4.63	3.94	4.12	0.96
TridentSE	Complex	3.47	4.70	3.81	4.10	0.96
MP-SENet (Reproduced)	Magnitude+Phase	3.56	4.69	3.92	4.20	0.96
MP-SENet w KAN (Ours)	Magnitude+Phase	3.61	4.73	3.92	4.25	0.96

distortion, overall quality and intelligibility of speech, respectively. For these speech quality metrics, higher scores indicate better performance. In addition, we compute the GFLOPs (FLOPs in billions) of the models when inference on a 10 second utterance. We also report the #P (M), the number of parameters in the models expressed in millions (M).

4.4. Experimental Results

Table 1 reports Demucs’s performance when the ReLU activations in the Encoder and/or Decoder are replaced with GR-KAN activations. In all runs, GR-KAN activations consistently outperform ReLU activations in all speech quality metrics, with approximately the same FLOPs and model size. The result shows the superiority of GR-KAN over ReLU activation in the time-domain Demucs.

Table 2 compares different GRU-Transformer variants in MP-SENet. The GR-KAN variant (Figure 2b) outperforms the Leaky ReLU and GELU variants at similar model size and FLOPs, suggesting GR-KAN activation’s stronger modeling capacity in the T-F domain MP-SENet. The original GRU-Transformer block in MP-SENet (LeakyReLU*) achieves the lowest performance, likely because it uses only one linear layer after the Bi-GRU module, compared to two layers in other runs.

Table 3 compares different decoder variants in MP-SENet, while the GRU-Transformer variant is fixed to the GR-KAN variant in Table 2. We observe that the decoders using KAN-Conv2D with both RBF-KAN and Swish activation (Figure 2c) have the best performance. When RBF-KAN activation in KAN-Conv2D is replaced with another Swish activation, there is a significant drop in PESQ from 3.609 to 3.537, indicating that the information captured by the RBF-KAN activation effectively complements the Swish activation. When KAN-Conv2D is replaced with Conv2D preceded by PReLU (the original implementation in MP-SENet), there is a drop in PESQ from 3.609 to 3.572, suggesting the stronger modeling capability of the KAN-Conv2D module.

Table 4 compares our KAN adapted MP-SENet against several well-known SE solutions on the VoiceBank-DEMAND dataset. Our method achieves the highest PESQ of 3.61, showing its superiority as a state-of-the-art SE method.

5. Conclusion

This work investigates KAN, a competitive alternative to MLP on the SE domain, by adapting 2 novel KAN variants based on rational function and radial basis function to existing SE solutions. Comprehensive experiments on the VoiceBank-DEMAND dataset demonstrate that these KAN variants surpass traditional MLPs with standard activation functions in both the time-domain Demucs and the T-F domain MP-SENet, with minimal or negligible increases in model size and computational cost. The encouraging results suggest that future SE approaches could benefit from incorporating KAN to achieve enhanced performance.

6. References

- [1] S. Pascual, A. Bonafonte, and J. Serra, “Segan: Speech enhancement generative adversarial network,” *arXiv preprint arXiv:1703.09452*, 2017.
- [2] A. Defossez, G. Synnaeve, and Y. Adi, “Real time speech enhancement in the waveform domain,” *arXiv preprint arXiv:2006.12847*, 2020.
- [3] E. Kim and H. Seo, “Se-conformer: Time-domain speech enhancement using conformer,” in *Interspeech*, 2021, pp. 2736–2740.
- [4] C. Chen, N. Hou, D. Ma, and E. S. Chng, “Time domain speech enhancement with attentive multi-scale approach,” in *2021 Asia-Pacific Signal and Information Processing Association Annual Summit and Conference (APSIPA ASC)*. IEEE, 2021, pp. 679–683.
- [5] Z. Wang, X. Zhu, Z. Zhang, Y. Lv, N. Jiang, G. Zhao, and L. Xie, “Selm: Speech enhancement using discrete tokens and language models,” in *ICASSP 2024-2024 IEEE International Conference on Acoustics, Speech and Signal Processing (ICASSP)*. IEEE, 2024, pp. 11 561–11 565.
- [6] S.-W. Fu, C.-F. Liao, Y. Tsao, and S.-D. Lin, “Metricgan: Generative adversarial networks based black-box metric scores optimization for speech enhancement,” in *International Conference on Machine Learning*. PmLR, 2019, pp. 2031–2041.
- [7] R. Cao, S. Abdulatif, and B. Yang, “Cmgan: Conformer-based metric gan for speech enhancement,” *arXiv preprint arXiv:2203.15149*, 2022.
- [8] V. Zadorozhnyy, Q. Ye, and K. Koishida, “Scp-gan: Self-correcting discriminator optimization for training consistency preserving metric gan on speech enhancement tasks,” *arXiv preprint arXiv:2210.14474*, 2022.
- [9] F. Dang, H. Chen, and P. Zhang, “Dpt-fsnet: Dual-path transformer based full-band and sub-band fusion network for speech enhancement,” in *ICASSP 2022-2022 IEEE International Conference on Acoustics, Speech and Signal Processing (ICASSP)*. IEEE, 2022, pp. 6857–6861.
- [10] D. Yin, Z. Zhao, C. Tang, Z. Xiong, and C. Luo, “Tridentse: Guiding speech enhancement with 32 global tokens,” *arXiv preprint arXiv:2210.12995*, 2022.
- [11] S.-W. Fu, C. Yu, T.-A. Hsieh, P. Plantinga, M. Ravanelli, X. Lu, and Y. Tsao, “Metricgan+: An improved version of metricgan for speech enhancement,” *arXiv preprint arXiv:2104.03538*, 2021.
- [12] Y.-X. Lu, Y. Ai, and Z.-H. Ling, “Explicit estimation of magnitude and phase spectra in parallel for high-quality speech enhancement,” *arXiv preprint arXiv:2308.08926*, 2023.
- [13] D. Michelsanti and Z.-H. Tan, “Conditional generative adversarial networks for speech enhancement and noise-robust speaker verification,” *arXiv preprint arXiv:1709.01703*, 2017.
- [14] A. Pandey and D. Wang, “On adversarial training and loss functions for speech enhancement,” in *2018 IEEE International Conference on Acoustics, Speech and Signal Processing (ICASSP)*. IEEE, 2018, pp. 5414–5418.
- [15] A. W. Rix, J. G. Beerends, M. P. Hollier, and A. P. Hekstra, “Perceptual evaluation of speech quality (pesq)-a new method for speech quality assessment of telephone networks and codecs,” in *2001 IEEE international conference on acoustics, speech, and signal processing. Proceedings (Cat. No. 01CH37221)*, vol. 2. IEEE, 2001, pp. 749–752.
- [16] C. H. Taal, R. C. Hendriks, R. Heusdens, and J. Jensen, “An algorithm for intelligibility prediction of time-frequency weighted noisy speech,” *IEEE Transactions on audio, speech, and language processing*, vol. 19, no. 7, pp. 2125–2136, 2011.
- [17] D. Hendrycks and K. Gimpel, “Gaussian error linear units (gelus),” *arXiv preprint arXiv:1606.08415*, 2016.
- [18] P. Ramachandran, B. Zoph, and Q. V. Le, “Searching for activation functions,” *arXiv preprint arXiv:1710.05941*, 2017.
- [19] M. Won, S. Chun, O. Nieto, and X. Serra, “Data-driven harmonic filters for audio representation learning,” in *ICASSP 2020-2020 IEEE International Conference on Acoustics, Speech and Signal Processing (ICASSP)*. IEEE, 2020, pp. 536–540.
- [20] Y.-X. Lu, Y. Ai, and Z.-H. Ling, “Mp-senet: A speech enhancement model with parallel denoising of magnitude and phase spectra,” *arXiv preprint arXiv:2305.13686*, 2023.
- [21] T. Szandafá, “Review and comparison of commonly used activation functions for deep neural networks,” *Bio-inspired neurocomputing*, pp. 203–224, 2021.
- [22] Z. Liu, Y. Wang, S. Vaidya, F. Ruehle, J. Halverson, M. Soljačić, T. Y. Hou, and M. Tegmark, “Kan: Kolmogorov-arnold networks,” *arXiv preprint arXiv:2404.19756*, 2024.
- [23] C. Li, X. Liu, W. Li, C. Wang, H. Liu, Y. Liu, Z. Chen, and Y. Yuan, “U-kan makes strong backbone for medical image segmentation and generation,” *arXiv preprint arXiv:2406.02918*, 2024.
- [24] X. Han, X. Zhang, Y. Wu, Z. Zhang, and Z. Wu, “Kan4tsf: Are kan and kan-based models effective for time series forecasting?” *arXiv preprint arXiv:2408.11306*, 2024.
- [25] K. Xu, L. Chen, and S. Wang, “Kolmogorov-arnold networks for time series: Bridging predictive power and interpretability,” *arXiv preprint arXiv:2406.02496*, 2024.
- [26] Y. Mai and S. Goetze, “Metricgan+ kan: Kolmogorov-arnold networks in metric-driven speech enhancement systems,” *channels*, vol. 5, p. 5.
- [27] A. N. Kolmogorov, “On the representation of continuous functions of many variables by superposition of continuous functions of one variable and addition,” in *Doklady Akademii Nauk*, vol. 114, no. 5. Russian Academy of Sciences, 1957, pp. 953–956.
- [28] X. Yang and X. Wang, “Kolmogorov-arnold transformer,” *arXiv preprint arXiv:2409.10594*, 2024.
- [29] Z. Li, “Kolmogorov-arnold networks are radial basis function networks,” *arXiv preprint arXiv:2405.06721*, 2024.
- [30] C. Valentini-Botinhao, X. Wang, S. Takaki, and J. Yamagishi, “Investigating rnn-based speech enhancement methods for noise-robust text-to-speech,” in *SSW*, 2016, pp. 146–152.
- [31] C. Veaux, J. Yamagishi, and S. King, “The voice bank corpus: Design, collection and data analysis of a large regional accent speech database,” in *2013 international conference oriental COCODA held jointly with 2013 conference on Asian spoken language research and evaluation (O-COCODAS/CASLRE)*. IEEE, 2013, pp. 1–4.
- [32] J. Thiemann, N. Ito, and E. Vincent, “The diverse environments multi-channel acoustic noise database (demand): A database of multichannel environmental noise recordings,” in *Proceedings of Meetings on Acoustics*, vol. 19, no. 1. AIP Publishing, 2013.
- [33] I. Loshchilov and F. Hutter, “Decoupled weight decay regularization,” *arXiv preprint arXiv:1711.05101*, 2017.
- [34] Y. Hu and P. C. Loizou, “Evaluation of objective quality measures for speech enhancement,” *IEEE Transactions on audio, speech, and language processing*, vol. 16, no. 1, pp. 229–238, 2007.